VOL.39 Nº2 2022
https://doi.org/10.22491/IMECTA.10852.en

Dimensionality Reduction by Signal-Dependent Adaptive Linear Transformation Applied to STAP Radars

Carlos Cypriano Vallim Junior*[a], Felipe Aurélio Caetano de Bastos[b], José Antonio Apolinário Junior[b]
[a]Centro de Avaliações do Exército (CAEx)
[b]Instituto Militar de Engenharia
Praça General Tibúrcio, 80, 22290-270, Praia Vermelha, Rio de Janeiro, RJ, Brasil.
***ccvallimjr@yahoo.com.br**

ABSTRACT: One of the key applications of space-time adaptive processing (STAP) is the detection of targets by surveillance radar systems, most notably by airborne radars and possibly in presence of strong interference signals. Notwithstanding, the ever growing number of elements used to build phased array antennas yields an amount of processing data that prevents practical implementation of full-rank processing and imposes a limit to the applicability of reduced-rank techniques as far as hardware technology and real-time systems requirements are concerned. This work proposes the application of an adaptive and signal dependent reduced-rank linear transformation (RLT) method to radar systems space-time processing. One will verify the computational complexity reduction resulting from the application of the method, as well as its performance in terms of STAP metrics, will be compared with other established reduced-rank techniques available in the literature. In order to verify its performance, the application of the RLT method to STAP radar systems will be employed on a scenario with a fixed platform, in presence of strong clutter and jamming scenario.

KEYWORDS: Space-time Adaptive Processing (STAP). Reduced-rank processing. Multistage Wiener filter. Householder reflectors. Planar array. Fixed platform radar.

RESUMO: Uma das principais aplicações do processamento adaptativo de espaço-tempo (space-time adaptive processing – STAP) é a detecção de alvos por sistemas de radar de busca e vigilância, notadamente para radares aerotransportados e possivelmente em presença de sinais interferentes fortes. Todavia, o crescente número de elementos empregados na construção de arranjos de antenas (phased array antennas) produz um volume de dados de processamento que inviabiliza a implementação prática de processamento de posto completo e limita a aplicabilidade de técnicas de posto reduzido quando são considerados a atual tecnologia de hardware e os requisitos de sistemas de tempo-real. Este trabalho se propõe a pesquisar e especializar um método de redução de posto por transformação linear (reduced-rank linear transformation – RLT) adaptativa, dependente de sinal, ao processamento de espaço-tempo de sistemas de radar. Verificar-se-á a redução de complexidade computacional resultante da aplicação do método RLT selecionado, bem como seu desempenho em termos de outras métricas do STAP, o qual será comparado com outras técnicas de redução de posto disponíveis na literatura. A fim de verificar seu desempenho, a aplicação do método RLT ao STAP será empregada no cenário de uma plataforma radar fixa em presença de clutter e jamming intensos.

PALAVRAS-CHAVE: Processamento Adaptativo de Espaço-tempo (STAP). Processamento em posto reduzido. Filtro de Wiener multiestágios. Refletores de Householder. Arranjo planar. Radar de plataforma fixa.

1. Introduction

Space-time processing, usually referred to as as space-time adaptive processing (STAP), is used in detection problems, tracking and radar censoring [1]. The STAP consists of the conjunct exploration of the spatial (angular) and temporal dependence (Doppler deviation) of the targets detected by a radar system and the cancelled interfering signals, to improve performance in the processing of radar signals compared to the conventional signal processing, i.e., spatial filtering and temporal filtering, sequential and separate.

Although the signal processing from a conventional radar system is sufficient for the suppression of fixed targets by fixed radar platforms, the use of 2D (two-dimensional) processing — the STAP — by a fixed radar, such as an aerial surveillance radar, remains attractive in the presence of interferences, whose statistical parameters are unknown *a priori*, as experimentally demonstrated in [2]. The application of STAP by a fixed platform in the presence of high levels of interference remains little explored in the literature. Combined with the potential application in fixed military and civilian radar projects in progress or in medium and long term, this fact may lead to further studies in this scenario.

The problem of reducing the size of received data in space-time processing increasingly attracts the interest of new research, given that the growing number of sensor elements in antenna arrangements produces challenging volumes of data for signal processing, especially when considering the application in systems operating in real-time. However, another relevant motivation, which also directs current research to the problem of reduced rank processing, lies in the scarcity of supporting data for the estimation of statistical parameters in realistic environments, resulting from the intrinsically non-stationary character of the clutter radar component that limits the amount of data available to estimate the statistical parameters of environmental interference, during the illumination period of the target by radar [3]. Some reduced rank techniques are capable of overcoming, in specific scenarios, the insufficiency of support data that are uncorrectable to the target sign of interest to estimate the covariance matrix of the interferences. Due to the application of these techniques, this matrix becomes invertible, enabling the filtering of space-time. Moreover, in some situations low-rank techniques result in performance than full-rank techniques [3]. Some rank reduction algorithms attract a lot of interest given their superior performance, in certain applications and under certain circumstances, to full-rank techniques and their capability to enable practical applications [4], [5]. A statistical rank reduction technique by adaptive linear transformation popularly applied by beamforming applications is the multistage Wiener filter (MWF) [6], [5]. An efficient implementation of the block matrix technique can be achieved by employing the Householder transformation [7]-[9].

This article aimed to specialize a technique of rank reduction by reduced-rank linear transformation (RLT) adaptive signal-dependent for the inversion of the covariance matrix of interferences, in order to enable the STAP in radar systems. We expected a reduction in computational complexity and performance gain regarding full rank techniques for estimation of covariance. The specialization of the proposed technique will be individualized for the scenario of fixed radar systems in the presence of high levels of interference, aiming for future practical applications.

This article presents: the space-time signal model applied to a scenario with side-looking airborne radar equipped with uniform linear array (ULA), and the STAP processor of interest (section 2); the householder multistage Wiener filter (HMWF), a filtering method of reduced rank applied to the STAP processing of a mobile radar with ULA (section 3); the application of the HMWF method, of reduced rank, to a fixed radar with uniform rectangular arrangement (URA) (section 4); the results of the implemented simulations (section 5); and the discussion of some conclusions, highlighting the contributions achieved (section 6).

2. Signal modelling for ULA

During the processing of the patterned radar receiver (Fig. 1), all space-time filtering is performed in the "STAP" stage, in which the output, $Z[l]$, is compared to a detection threshold.

Considering a mobile *phased-array* STAP radar with a uniform linear arrangement (ULA), with N elements and coherent processing interval (CPI) that integrates coherent M pulses (or slow-time samples). The pulse repetition interval is sampled with rate, $1/L$, where L is the number of fast-time samples.

The radar transmitter emits a pulsed waveform, $\boldsymbol{S_{TX}(t)}$. The analytical echo signal received by the nth reception channel, relative to the target of interest and converted to baseband is given by the expression [3], [10]

VOL.39 Nº2 2022
https://doi.org/10.22491/IMECTA.10852.en

$$S_{RX}(t) = \frac{A_{tgt}}{\sqrt{2}} e^{j\psi} S_{TX}(t - \tau_{tgt}) e^{j2\pi\vartheta_{tgt}} e^{j2\pi f_{tgt} t} \quad (1)$$

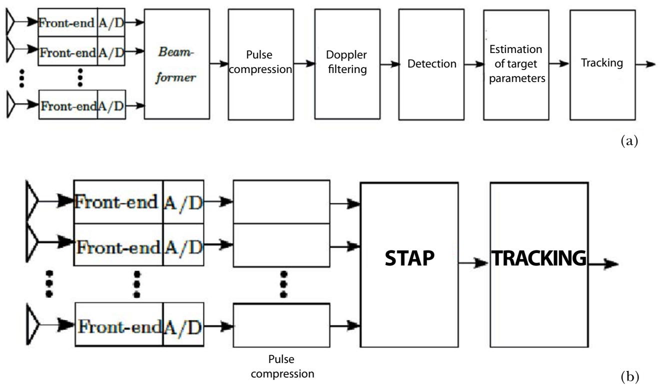

Fig. 1 - Comparison between block diagrams of (a) a Conventional Radar Processor and (b) a Radar STAP Processor.

where A_{tgt} is the amplitude of the echo, τ_{tgt} is the electromagnetic propagation delay, which covers the time from the emission of the pulsed waveform to the reception of the echo signal, $\psi = -2\pi\left(f_c + f_{tgt}\right)\tau_{tgt}$, f_c, is the frequency of the carrier, f_{tgt} is the Doppler frequency due to the target spatial movement, $\vartheta_{tgt}(\theta_{tgt}, \phi_{tgt}) = \frac{d}{\lambda_c} \cos\theta_{tgt} \operatorname{sen} \phi_{tgt}$ is the spatial frequency of the target, θ_{tgt} and ϕ_{tgt} are, respectively, the elevation and azimuth angles of the target. Echo signals are subjected to matched filters on each channel for pulse compression. After data compression, the echo signal is given by [3], [10]

$$\chi_{mn}(t) = \beta_{tgt} e^{j2\pi\vartheta_{tgt}(\theta_{tgt},\phi_{tgt})} e^{j2\pi f_{tgt} \frac{m}{PRF}} \times$$
$$\chi\left(t - \tau_{tgt} - \tau_p - \frac{m}{PRF}, 0\right) \begin{cases} n = 0, 1, \cdots, N-1 \\ m = 0, 1, \cdots, M-1 \end{cases} \quad (2),$$

where $\beta_{tgt} = \left(A_{tgt}/\sqrt{2}\right) e^{-j2\pi f_c \tau_{tgt}}$ is the width of each pulse (τ_p), and $\chi(t, f)$ the ambiguity function of the matched filter implemented by the radar receiver detection stage. The compressed signal is sampled in the instants $\chi_{mn}(t)$ and $t = t_0 + 1/f_s + m/PRF$, where t_0 is the initial instant of the l-th range gate, $l = 0, 1, \cdots, L-1$ and $f_s > 2B_p = 2c/2\Delta R$ is the sampling frequency of the interval between successive pulses (PRI), B_p is the pulse bandwidth and ΔR the resolution in radar range. Therefore, the sampled signal can be expressed as [3], [10]

$$x_{mn}[l] = \zeta_l e^{j2\pi\vartheta_{tgt}} e^{\frac{j2\pi f_{tgt} m}{PRF}}, \begin{cases} n = 0, 1 \cdots, N-1; \\ m = 0, 1 \cdots, M-1; \\ l = 0, 1 \cdots, L-1, \end{cases} \quad (3),$$

where $\zeta_l = \beta_{tgt} \chi(t_0 - lf_s - \tau_{tgt} - \tau_p, 0)$. The amplitude of the signal described by the previous equation is maximum when $t = t_0 + 1/f_s \approx \tau_{tgt} + \tau_p$, that is, equivalent to the maximization of $|x_{mn}[l]|$ when the l-th *range gate* corresponds to the range of the target of interest. Therefore, the compressed signal, $x_{mn}[l]$, corresponds to the nm-th element of the l-th *snapshot* of the considered CPI space-time, which composes the input data of the STAP filter.

The detailing of simplified modelling for interferences (clutter, jamming, and noise) can be found in [10].

The space-time snapshot received by the sensors arrangement correspondent to the l-th range gate, of dimension $M \times N$, is represented by its vectorization, $\mathbf{r}[l] \in \mathbb{C}^{MN \times 1}$ and described by the expression [3]

$$\mathbf{r}[l] = \alpha_{tgt}[l] \mathbf{s}(\vartheta_{tgt}, f_{tgt}) + \mathbf{i}[l] \quad (4),$$

where the signal component is $\alpha_{tgt}[l] \mathbf{s}(\vartheta_{tgt}, \varpi_{tgt})$. The space-time steering vector is given by $\mathbf{s}(\vartheta_{tgt}, \varpi_{tgt}) = \mathbf{a}(\vartheta_{tgt}) \otimes \mathbf{b}(\varpi_{tgt})$, and $\otimes$ indicates the product of Kronecker, where [3]

$$\mathbf{a}(\vartheta_{tgt}) = \left[1 e^{(-j2\pi\vartheta_{tgt})} \cdots e^{(-j2\pi(N-1)\vartheta_{tgt})}\right]^T \quad (5) \text{ and}$$
$$\mathbf{b}(\varpi_{tgt}) = \left[1 e^{(-j2\pi\varpi_{tgt})} \cdots e^{(-j2\pi(M-1)\varpi_{tgt})}\right]^T \quad (6) \text{ are,}$$

respectively, the spatial and temporal components [3], λc is the length of the carrier wave, d is the spacing between the elements of the arrangement of antennas, Φ_{tgt} is the azimuth angle of the target of interest and ϖ_{tgt} is the Doppler frequency, normalized according to the pulse repetition frequency (PRF) of the radar. The interference-plus-noise vector of space-time, $\boldsymbol{i}[l]$, results from the sum of interferences (clutter and jamming) and noise present in the l-th range gate.

The snapshots received by ULA are subjected to the space-time filter, $\mathbf{w} \in \mathbb{C}^{MN \times 1}$, producing complex scalar output [3]

$$z[l] = \mathbf{w}^{\mathrm{H}}\mathbf{r}[l] \qquad (7).$$

In order to maximize the probability of detection, *PD*, we applied the MVDR filter (minimum variance distortionless response) of space-time [3]

$$\mathbf{w}_{MVDR} = \frac{\mathbf{R}^{-1}\mathbf{s}}{\mathbf{s}^{\mathrm{H}}\mathbf{R}^{-1}\mathbf{s}} \qquad (8),$$

where $\boldsymbol{R} = E[\mathbf{r}[l]\mathbf{r}H[l]]$ is the total covariance matrix of interferences and $\mathbf{s} = \mathbf{a}(\vartheta_{tgt}) \otimes \mathbf{b}(\varpi_{tgt})$ is the steering vector of space-time.

We can demonstrate [10] that the expected value of the signal-plus-interference-to-noise ratio (SINR), normalized regarding the optimal SINR, $\mathrm{E}[\rho]$, is given by

$$\mathrm{E}[\rho] = \frac{K + 2 - MN}{K + 1}, \qquad (9)$$

where K is the number of support samples (space-time snapshots) processed by the filter. Solving the previous equation, making $K = 2MN$, for example, we obtained $E[\rho] \approx 0{,}5$, which results in a difference of approximately 3 dB between the filter SINR and the optimal SINR. When $K = MN$ the result is $E[\rho] = 2/(MN + 1)$. Even though the value of K is an inadequate support sample for the MVDR-SMI filter, the application of the HMWF filter can achieve a satisfactory performance with a sample quantity equal to or less than $K = MN$, as section 5 will present.

3. HMWF on STAP radar ULA mobile

In this section, the HMWF technique with rank reduction is specialized for space-time applications. As in the MWF method, HMWF achieves a rank r reduction by filter truncation in the r-th stage; however, the desired signal block is implemented by Householder reflectors, which are given by [7], [8], [9]

$$\mathbf{v}_i = \frac{|h_{i,1}|}{h_{i,1}}\mathbf{h}_i - \mathbf{u}_1 \qquad (10),$$

where $\mathbf{h}_i$ is the normalization of the cross-correlation between the reference signal and the *snapshots* of the i-th stage of the filter, which is colinear to the direction of the sign of interest, and $h_{i,1}$ is the first element of the vector $\mathbf{h}_i$. Householder reflectors have a unitary standard and produce a rotation around the first element of the unit vector in the direction of the sign of interest. In Eq. (10), $\mathbf{u}_1 = [1 0 \cdots 0]^{\mathrm{T}}$. With the reflectors, householder matrix is constructed as follows [9]

$$\mathbf{H}_i = \frac{|h_{i,1}|}{h_{i,1}}\left(\mathbf{I} - 2\frac{\mathbf{v}_i\mathbf{v}_i^{\mathrm{H}}}{\mathbf{v}_i^{\mathrm{H}}\mathbf{v}_i}\right) \qquad (11).$$

We can easily demonstrate that the Householder matrix is unitary, i.e., $\mathbf{H}^{\mathrm{H}}\mathbf{H} = \mathbf{H}\mathbf{H}^{\mathrm{H}} = \mathbf{I}$, where $\boldsymbol{I}$ is the identity, and its first column is $\mathbf{h}_i$ [9]. These two properties imply that the block matrices, $\mathbf{b}_i$,, are obtained from the other columns of the Householder array, i.e., $\mathbf{H}_i = [\mathbf{h}_i\mathbf{B}_i]$.

The HMWF technique applies to a STAP side looking airborne phased-array radar with ULA, N elements and CPI, which integrates M coherent pulses of the same modelling as in section 2, also operating subjected to the same interference conditions.

The rank reduction techniques, including the HMWF filter, can circumvent the restrictions imposed by reduced support samples in estimating the space-time covariance matrix. The application of the HMWF results in a reduced rank space-time filter, $\mathbf{w}_{HMWF}$, given by

$$\mathbf{w}_{HMWF} = \frac{\mathbf{R}_r^{-1}\mathbf{s}_r}{\mathbf{s}_r^{\mathrm{H}}\mathbf{R}_r^{-1}\mathbf{s}_r} \qquad (12),$$

where $\mathbf{R}_r = \mathbf{T}_{HMWF}^{\mathrm{H}}\mathbf{R}\mathbf{T}_{HMWF} = \mathrm{E}[\mathbf{x}_r[l]\mathbf{x}_r^{\mathrm{H}}[l]]$ is the covariance matrix of interferences after the rank reduction, $\mathbf{T}_{HMWF}$ is the linear transformation matrix of rank reduction, $\mathbf{x}_r[l] = \mathbf{T}_{HMWF}^{\mathrm{H}}\mathbf{x}[l]$, and $\mathbf{s}_r = \mathbf{T}_{HMWF}^{\mathrm{H}}\mathbf{s}$ is the steering vector of space-time of the signal received after the rank reduction.

4. HMWF on fixed URA STAP radar

Similarly to the preceding section, the STAP filter of reduced rank by HMWF technique implemented on the receiver of a fixed radar with uniform rectangular arrangement will be modeled. We considered a terrestrial phased-array radar STAP, with URA composed of N elements, integrating M coherent pulses and being constructed according to the geometry presented in Fig. 2, whose CPI is schematized in Fig. 3. The CPI is composed of L snapshots with $M \times N$ dimension *space-time,* represented by vectors $\mathbf{r}[l] \in \mathbb{C}^{MN\times 1}$, given by the same expression as Eq. (1). The space-time steering vector results from the Kronecker product of the temporal steering vector, of dimension $M \times 1$, given by (6), via the spatial *steering vector* dimension $N \times 1$, given by (5), and that

$$\boldsymbol{\vartheta}_{tgt}(\theta_{tgt}\phi_{tgt}) = \left[\vartheta_0(\theta_{tgt}\phi_{tgt})\vartheta_1(\theta_{tgt}\phi_{tgt}) \cdots \vartheta_{N\text{-}1}(\theta_{tgt}\phi_{tgt})\right] \tag{13}$$

is the vector $N \times 1$ that gathers the spatial frequencies of the target regarding each element of the arrangement.

To rank reduction, we apply the HMWF algorithm to the MVDR space-time filter to obtain a reduced rank space-time filter, whose number of HMWF stages gives new dimensionality, as in the Eq. (12). The covariance matrix is obtained from the space-time snapshots, whose components modelling of the echo signal and interferences (jamming, clutter and noise) is analogous to the scenario with ULA, replacing it in the Eq. (4) to (6) the spatial frequency of the linear arrangement, ϑ_{tgt}, by spatial frequencies, $\vartheta(\theta_{tgt}\phi_{tgt})$ corresponding to each of the N elements of the URA (i.e., the elements of the vector $\boldsymbol{\vartheta}_{tgt}$).

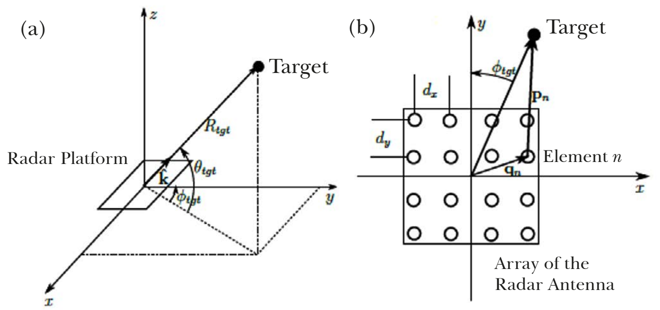

Fig. 2 - (a) Geometry of the radar platform with URA. (b) Top view.

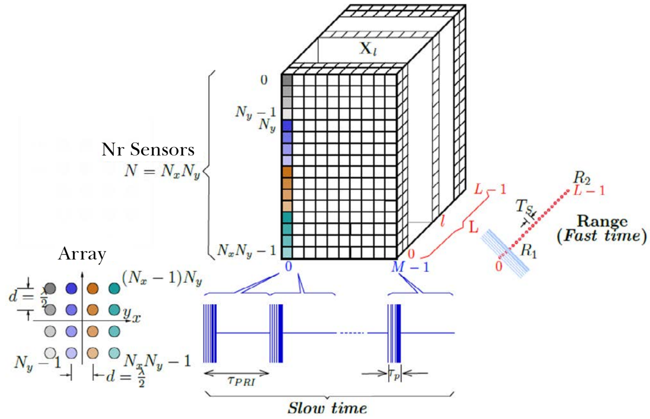

Fig. 3 - Coherent processing interval (CPI).

5. Simulations

This section presents simulation results using MVDR sample matrix inversion algorithms [3] of reduced rank, in a scenario with scarce support samples. The reduced rank algorithms for performance comparison with HMWF in the proposed application are: principal components (PC) [11], [12], cross-spectral metric (CSM) [13], [14], [15], and MWF [6].

According to the details in [10], a mobile airborne phased-array radar equipped with ULA, and a fixed terrestrial phased-array radar with URA were simulated. Antenna arrangements of both radars have a total of elements $N = 16$ with a half carrier wavelength spacing. The radars transmit $M = 40$ pulses per CPI, totaling $MN = 640$ degrees of freedom adaptive from the space-time filter. Both radars have a carrier frequency of 1 GHz, PRF of 2.5 kHz, pulse duration of 20 μs, peak transmission power of 700 W, maximum interest range of 60 km, maximum interest speed of 187 m/s, and resolution at a speed of 9.4 m/s. The simulated target has a Doppler frequency of 400 Hz and is 10 km far from the radar position. Both scenarios, i.e. mobile ULA and fixed URA, simulate an interference that produces a jammer-noise ratio (JNR) per element of 40 dB, and the noise is assumed stationary gaussian white of zero mean.

VOL.39 Nº2 2022
https://doi.org/10.22491/IMECTA.10852.en

The airborne radar travels at approximately 187 m/s along the direction defined by the ULA elements and has a resolution at a range of 25 m. In this scenario, uniform clutter was inserted along 360° of azimuth, with clutter-noise ratio (CNR), per element and pulse, of 50 dB, without ambiguity in the Doppler spectrum, misalignment of the platform velocity vector and intrinsic movement of the clutter.

The terrestrial radar is fixed on the ground and has a resolution at a range of 75 m. In the scenario with the fixed URA radar, the clutter was synthesized and evenly distributed in azimuth in the quadrant between the azimuth 0° and 90° and, in range, between 10.5 km and 11.5 km, with CNR of 50 dB, without ambiguities.

Fig. 4 presents the normalized SINR behavior in relation to optimal SINR for the application of HMWF to the MVDR-SMI filter. In this figure, the number of samples was varied for both scenarios (ULA and URA). We compared the HMWF performance with MWF, CSM, PC, and quiescent filter ($\boldsymbol{w} = \boldsymbol{S}$), applied to MVDR-SMI.

Similarly, using the probability of detection (P_D) and the probability of false alarm (P_{FA}), as defined in [1], the performance of the HMWF application to the MVDR-SMI was compared to the other techniques of the previous simulation, obtaining the result presented in Fig. 5.

Regarding computational complexity, using the expressions in Table 1, Fig. 6 was obtained by varying the number of stages (rank) of the filters and using 640 support samples.

Table 1 - Computational complexity of HMWF and MWF.

Algorithm	Complex multiplications
MVDR-SMI full rank	$K(2M^3N^3 + 13M^2N^2 + 9MN)/3$
MWF	$Kr^3/3 - KMNr^2 + K(M^2N^2 - 1/3)r$
HMWF	$-Kr^3/3 + K(MN/2 - 5)r^2 + K(13/6 + M^2N^2/2 + 11MN/2)r - 6KMN - K$

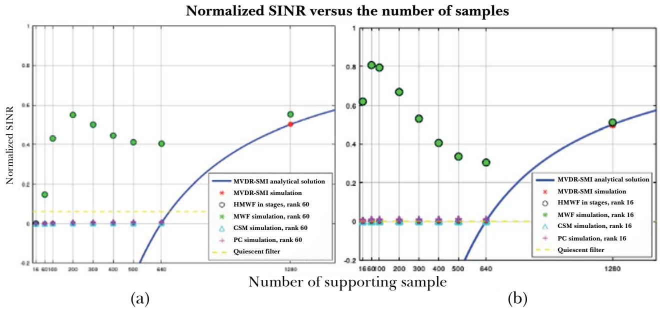

Fig. 4 – Normalized SINR versus the number of support samples, K, of HMWF, $M = 40$, $N = 16$, 100 Monte Carlo iterations. (a) Mobile ULA radar, rank $r = 55$. (b) Fixed URA radar, rank $r = 16$.

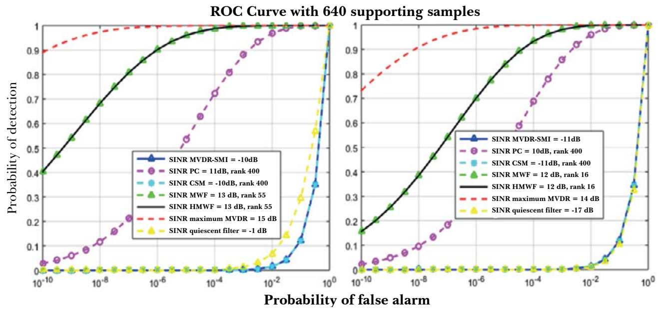

Fig. 5 - P_D versus P_{FA} (ROC Curve), $K = MN = 640$, 100 Monte Carlo iterations. (a) Mobile ULA radar, rank $r = 55$. (b) Fixed URA radar, rank $r = 16$.

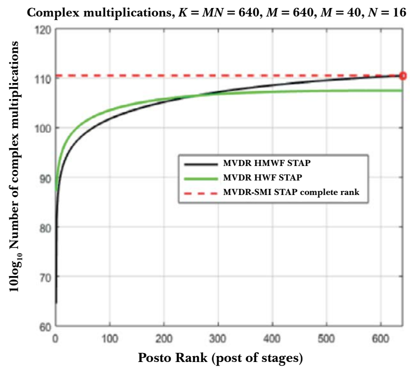

Fig. 6 - Number of complex multiplications versus the number of stages (rank) of HMWF and MWF algorithms, $K = MN = 640$ support samples.

6. Conclusion

This article explored the application of HMWF (householder multistage Wiener filter) by phased-array radars in two scenarios: a side looking airborne radar equipped with a ULA and a fixed ground radar with URA. By applying the HMWF to the STAP, the same performance was obtained as the conventional MWF, especially regarding the capacity of operating with a rank reduction of up to 128 times regarding the complete rank, even for a small number of support samples. Moreover, comparing to the other techniques simulated and available in the literature, for the metrics used in performance simulations, the reduced operating capacity of the HMWF is significantly higher.

Furthermore, the application of HMWF to STAP confirmed a higher computational efficiency for reduced rank and number of samples. This promising result meets one of the main current research objectives in the field of radar space-time processing, assuming the scarcity of samples containing stationary interferences regarding the snapshot that STAP filtering is intended to be applied.

References

[1] RICHARDS, M. A. Fundamentals of Radar Signal Processing. 2. ed. New York: McGraw-Hill Professional, 2014.

[2] FARINA, A.; TIMMONERI, L. Cancellation of clutter and E.M. Interference with STAP algorithms. Application to live data acquired with a ground-based phased-array radar. In IEEE Radar Conference. Piscataway: IEEE, 2004.

[3] WARD, J. Space-time adaptive processing for airborne radar. Technical Report 1015. Lexington, MA: Massachussetts Institute of Technology, 1994.

[4] HIEMSTRA, J. D.; GOLDSTEIN, J. S. Robust rank selection for the multistage Wiener filter. In IEEE International Conference on Acoustics, Speech and Signal Processing (ICASSP 2002). Piscataway: IEEE, 2002.

[5] OLIVEIRA, A.; SAMPAIO-NETTO, R.; FORTES, J. M.; BACKX, F. Interpolation-and-decimation-based dimensionality reduction applied to space-time processing. In IEEE Sensor Array and Multichannel Signal Processing Workshop (SAM). Piscataway: IEEE, 2016. p. 1–5.

[6] GOLDSTEIN, J. S.; REED, I. S.; SCHARF, L. L. A multistage representation of the Wiener filter based on orthogonal projections. IEEE Transactions on Information Theory, v. 44, n. 7, p. 2943–2959, 1990.

[7] CAMPOS, M. L. R.; WERNER, S.; APOLINÁRIO JR, J. A. On an efficient implementation of the multistage Wiener filter through Householder reflections for DS-CDMA interference suppression. In IEEE Global Telecommunications Conference (GLOBECOM). Piscataway: IEEE, 2003.

[8] WERNER, S.; With, M.; KOIVUNEN, V. Householder multistage Wiener filter for space-time navigation receivers. IEEE Transactions on Aerospace and Electronic Systems, v. 43, n. 3, p. 975–988, 2007.

[9] YANG, X.; SUN, Y.; LIU, Y.; ZHANG, J. Derivative constraint-based Householder multistage Wiener filter for adaptive beamforming. In IET International Radar Conference. Auburn Hills, MI: IET Internacional, 2013. p. 1–5.

[10] VALLIM JR, C. C. Redução de Dimensionalidade por Transformação Linear Adaptativa Dependente de Sinais Aplicada a Radares STAP. Dissertação (Mestrado em Ciências em Engenharia Elétrica) – Instituto Militar de Engenharia, Rio de Janeiro, 2018.

[11] HOTELLING, H. Analysis of a complex of statistical variables into principal components. Journal of Educational Psychology, v. 24, n. 6, p. 417–441, 1933.

[12] HAIMOVICH, A. The eigencanceler: adaptive radar by eigenanalysis methods. Aerospace and Electronic Systems. IEEE Transactions on Aerospace and Electronic Systems, v. 32, n. 2, p. 532–542, 1996.

[13] GOLDSTEIN, J. S.; REED, I. S. Reduced rank adaptive filtering. IEEE Transactions on Signal Processing, v. 45, n. 2, p. 492–496, 1997.

[14] GOLDSTEIN, J. S.; REED, I. S. Theory of partially adaptive radar. IEEE Transactions on Aerospace and Electronic Systems, v. 33, n. 4, p. 1309–1325, 1997.

[15] GOLDSTEIN, J. S.; REED, I. S.; ZULCH, P.; MELVIN, W. A multistage STAP CFAR detection technique. In IEEE Radar Conference (RADARCON). Piscataway: IEEE, 1998.